Cellular and Molecular Life Sciences (2020) 77:3265–3277
https://doi.org/10.1007/s00018-019-03354-4

ORIGINAL ARTICLE

Genetic deletion of a short fragment of glucokinase in rabbit by CRISPR/Cas9 leading to hyperglycemia and other typical features seen in MODY-2

Yuning Song[1] · Tingting Sui[1] · Yuxin Zhang[1] · Yong Wang[1] · Mao Chen[1] · Jichao Deng[1] · Zhonglin Chai[2] · Liangxue Lai[1] · Zhanjun Li[1]

Received: 26 February 2019 / Revised: 22 October 2019 / Accepted: 23 October 2019 / Published online: 13 November 2019

Abstract

Glucokinase (*GCK*) is a key enzyme in glucose sensing and glycemic regulation. In humans, mutations in the *GCK* gene cause maturity-onset diabetes of the young 2 (MODY-2), a disease that is characterized by an early-onset and persistent hyperglycemia. It is known that *Gck* knockout (KO) is lethal in mice with *Gck* KO mice dying within 2 weeks after birth. Therefore, *Gck* KO mice are not suitable for preclinical study and have limited suitability to study the pathophysiological role of glucokinase in vivo. Here, we report the generation of a novel rabbit with a non-frameshift mutation of *GCK* gene (*GCK*-NFS) by cytoplasm microinjection of Cas9 mRNA and gRNA. These *GCK*-NFS rabbits showed typical features of MODY-2 including hyperglycemia and glucose intolerance with similar survival rate and weight compared to wild-type (WT) rabbits. The diabetic phenotype including pancreatic and renal dysfunction was also found in the F1-generation rabbits, indicating that the genetic modification is germline transmissible. Treatment of *GCK*-NFS rabbit with glimepiride successfully reduced the fasting blood glucose drastically and improved its islet function. In conclusion, this novel *GCK* mutant rabbit generated with the CRISPR/Cas9 system mimics most, if not all, histopathological and functional defects seen in MODY-2 patients such as hyperglycemia and will be a valuable rabbit model for preclinical studies and drug screening for diabetes as well as for studying the pathophysiological role of glucokinase.

Keywords Glucokinase · MODY-2 type · Rabbit · CRISPR/Cas9 · Preclinical testing

Introduction

The *GCK* gene (7p15.3-p15.1) encodes the enzyme glucokinase, a 465-amino acid protein which plays a major role in glycolysis [1]. Glucokinase acts as a glucose sensor and contributes to maintaining glucose homeostasis through glucose-stimulated insulin secretion [2]. Mutations of *GCK* have been widely reported in Maturity-onset diabetes of the young 2 (MODY-2) patients, which is a clinically heterogeneous group of disorders characterized by nonketotic diabetes mellitus, with onset usually before the age of 25 years (frequently in childhood or adolescence) and a primary defect in the function of the beta cells of the pancreas [1]. Hyperglycemia in *GCK*-MODY-2 resulting from a *GCK* mutation leads to both a reduced sensitivity of β-cells to glucose and a defect in glycogen synthesis in liver, as a consequence of a decreased *GCK* activity [3]. To date, over 600 different *GCK*-MODY-2 mutations have been reported, including those which result in a frameshift and/

Yuning Song, Tingting Sui and Yuxin Zhang contributed equally to this work.

Electronic supplementary material The online version of this article (https://doi.org/10.1007/s00018-019-03354-4) contains supplementary material, which is available to authorized users.

✉ Liangxue Lai
lai_liangxue@gibh.ac.cn

✉ Zhanjun Li
lizj_1998@jlu.edu.cn

[1] Jilin Provincial Key Laboratory of Animal Embryo Engineering, Jilin University, Changchun 130062, China

[2] Department of Diabetes, Central Clinical School, Pathophysiology of Diabetic Complications Laboratory, Monash University, Melbourne, Australia

or a premature stop codon formation in the *GCK* gene, thus disrupting the expression of functional glucokinase from the affected allele [4, 5]. Due to the loss of *GCK* expression from the mutated allele, MODY-2 subjects have a reduced expression level of GCK, which can only be produced by the WT allele, leading to an overall reduced GCK activity per cell.

At present, only the *Gck* KO [6–8] and *Gck* transgenic mice [9–12] have been generated and used for preclinical studies. However, these *Gck* gene-modified mice have various phenotypes [13]. For example, a hepatocyte-specific *Gck* KO mouse showed a slight change in blood glucose (BG) [14], and the pancreatic β-cell-specific *Gck* KO mice showed more serious hyperglycemia and insulin resistance [15, 16]. Moreover, two different lines of *Gck* null mice differ markedly in their age of death; one is lethal at midgestation, whereas the other dies shortly after birth, thereby preventing using these mice as an adult disease model for detailed pathophysiological studies on *Gck* in disease [6]. Therefore, there is a need to develop a better animal model in other species with glucokinase mutations to study the in vivo role of glucokinase. Of note, the rabbits share more similarities with humans in terms of physiology, anatomy, and genetics than mouse [17]. It has a short gestation period (30–31 days), large litter size (4–12/l) and can be housed conveniently in an indoor facility. Furthermore, the manifestations of metabolic and cardiovascular diseases in rabbit are similar to those in human beings [18].

In this study, we established the first rabbit model with a non-frameshift (NFS) deletion of a fragment of 36 bp within the exon 3 of the *GCK* gene by cytoplasm microinjection of Cas9 mRNA and gRNA. These *GCK*-NFS rabbits showed typical features of MODY-2 including hyperglycemia, glucose intolerance and normal weight. Notably, the *GCK*-NFS rabbits are fertile and stably inherit the diabetic phenotypes in association with the mutant *GCK* genotype, suggesting that this model can be used for preclinical studies and investigation of the physiological and pathophysiological roles of *GCK* in the *GCK*-MODY syndrome.

Research design and methods

Ethics statement

The rabbits used in this study were New Zealand white rabbits. All animal studies were conducted according to experimental practices and standards approved by the Animal Welfare and Research Ethics Committee at Jilin University.

Vector construction and in vitro transcription

Vector construction and in vitro transcription were carried out as described previously [19]. Briefly, to produce sgRNA, two complementary DNA oligonucleotides were annealed at 95 °C for 5 min to generate double-strand DNA and then cloned into a BbsI-digested pUC57-simple vector expressing Cas9 (Addgene ID 51307).

Embryo collection, microinjection, and transfer

The protocol for microinjection of pronuclear-stage embryos has been described in detail in our published protocols [20]. Briefly, a mixture of Cas9 mRNA (200 ng/ul) and sgRNA (50 ng/ul) was co-injected into the cytoplasm of pronuclear-stage zygotes. These zygotes were then immediately transferred into the oviducts of surrogate rabbits.

Mutation and off-target effect detection assay

The protocol for the mutation and off-target effects detection assay has been described previously [21]. PCR primers are listed in Supplementary Table S1. PCR products were gel purified and cloned into pGEM-T vectors (Tiangen, China). Ten positive plasmid clones were sequenced, and DNAman was used for sequence analysis.

Real-time quantitative PCR (qRT-PCR)

The protocols for the RNA and cDNA isolation have been described in detail in our published papers [19, 21]. qRT-PCR was performed using the BIO-RAD iQ5 Multicolor Real-Time PCR Detection System with the BioEasy SYBR Green I Real-Time PCR Kit (Bioer Technology, Hangzhou, China) according to the manufacturer's instructions. The *GAPDH* was used as an internal control for normalization of individual samples. The relative gene expression was presented as mean ± S.E.M and analyzed by $2^{-\Delta\Delta CT}$ formula. Data were statistically analyzed by GraphPad Prism software (*T* test) and a $p < 0.05$ was considered as statistically significant. The primers used for qRT-PCR are shown in supplementary table S1.

Determination of metabolic data and biochemical analysis of biological samples

The survival rate of *GCK*-NFS and WT rabbits was recorded daily and body weight was recorded weekly. An intraperitoneal glucose tolerance test (IPGTT) and insulin tolerance test (ITT) were performed as described previously [22]. Blood samples were bled from the postorbital vein and sera

were prepared by separation of the serum from the clot following a brief centrifugation. The serum insulin levels were determined using an INS ELISA Kit (IBL, Germany). The C peptide levels were measured using a C-PEP ELISA Kit (IBL, Germany). The fructosamine, triglyceride (TG) and total cholesterol (TC) were measured by the Chinese People's Liberation Army 208 hospital via a contracted service.

Urine glucose was determined by the glucose oxidase method [14]. Urine protein concentrations were measured using a Coomassie dye-binding protein assay with bovine serum albumin as a standard. The concentrations of urine protein and glucose were calculated and all data are expressed as mean ± S.E.M.

T7 endonuclease I (T7EI) assay

A T7 endonuclease I (T7EI) assay was performed as described previously [23]. Briefly, the genomic DNA was extracted from either injected blastocysts or animal tissues as mentioned above. The regions containing the targeted site or the potential off-target sites were amplified by PCR with gene-specific primers (Table S2), then the PCR products were denatured and annealed under the following conditions: 95 °C for 5 min, 95 °C for 5 min, 95–85 °C at − 2 °C/s, 85–25 °C at − 0.1 °C/s, hold at 4 °C. The annealed samples were digested with T7EI (NEB M0302L), separated and measured on an ethidium bromide-stained 10% polyacrylamide TAE gel.

Histology

Hematoxylin and eosin (HE) stain [18]: briefly, eye, kidney, skeletal muscle, heart and liver tissues from *GCK*-NFS and WT rabbits were fixed with 4% paraformaldehyde for 48 h, embedded in paraffin and sectioned. Tissue sections were then stained with hematoxylin and eosin and examined by microscopy (Nikon ts100).

Periodic acid-schiff (PAS) stain [24]: tissue sections were stained by periodic acid-schiff (PAS) Stain to examine the glycogen deposition in kidney, skeletal muscle, heart and liver tissues. The staining quality and the glycogen content in these tissues were compared in the groups.

Masson's trichrome staining [25]: various tissues including eye, kidney, skeletal muscle, heart and liver tissues were collected from *GCK*-NFS and WT rabbits. The tissues were fixed in 4% paraformaldehyde at 4 °C, dehydrated in increasing concentrations of ethanol (70% for 6 h, 80% for 1 h, 96% for 1 h, and 100% for 3 h), cleared in xylene and embedded in paraffin for the histological examination. The 5-μm sections were cut for Masson's trichrome staining. The stained sections were imaged with a Nikon TS100 microscope.

Van Gieson's stain [26]: for identifying elastic fibers in tissues, paraffin sections were cut and deparaffinized with 96% ethanol. Sections were then stained with Weigert's Iron hematoxylin solution for 10 min, soaked under running water for approximately 30 min for destaining, and then stained with Van Gieson's stain for 15 min. The sections were examined by microscopy (Nikon ts100).

Toluidine blue stain [27]: for observation of osteoblasts, the bone sections were first incubated in diastase solution at 37 °C for 1 h and washed. The air-dried smear with bone sections was flooded with Toluidine blue stain for 1 min followed by washing in a stream of deionized water.

Bone structure and histomorphology

X-ray autoradiography pictures of femurs and tibias in *GCK*-NFS and WT rabbits were taken using the YEMA Radiography System with a digital camera attached (Varian, USA) on X-ray film (ROTANODE, Japan). The images were taken at 40 kV with 3-mAs exposure. Bone mineral density (BMD) was analyzed by Alpha View SA.

For histological analyses, femurs and tibias in *GCK*-NFS and WT rabbits were collected and the surrounding muscles were removed. The bones were then fixed in 4% paraformaldehyde at 4 °C, and subsequently decalcified in 15% EDTA for 2 weeks, dehydrated in progressive concentrations of ethanol (70% for 6 h, 80% for 1 h, 96% for 1 h and 100% for 3 h), washed with xylene and embedded in paraffin. Sections of 0.05 cm were cut and used for HE staining, Masson-staining and Toluidine blue as described above and were then analyzed by microscopy (Nikon ts100) [25].

Enzyme content and activity

For glucokinase content and activity measurements, the freeze-clamped liver and muscle of *GCK*-NFS and WT rabbits were homogenized in 50 mmol/l HEPES, 100 mmol/l KCl, 1 mmol/l EDTA, 5 mM MgCl2, and 2.5 mmol/l dithioerythritol. Glucokinase content and activities were determined in the supernatant and sedimentary fractions. After centrifugation at 20,000×*g* at 4 °C for 10 min, the supernatant was analyzed for the glucokinase activity by a glucokinase Colorimetric Assay Kit (Biovision Research Products, Mountain View, CA).

Statistical analyses

All data are expressed as mean ± S.E.M, of at least three individual determinations per parameter in all experiments. The data were analyzed with *t* test using GraphPad Prism software 6.0. A probability of $p < 0.05$ was considered statistically significant.

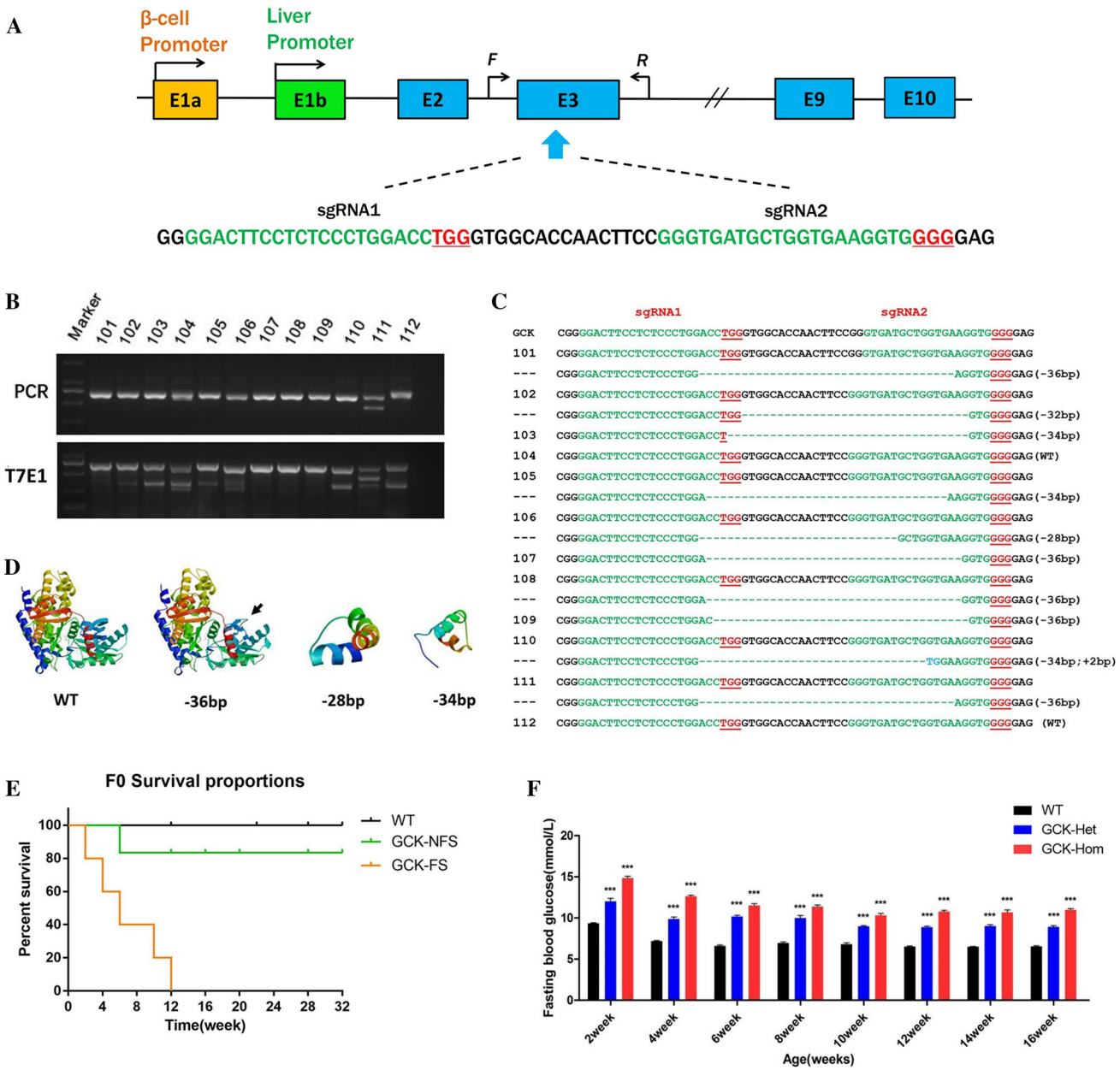

Fig. 1 Genome editing of the *GCK* gene via the Cas9/gRNA system. **a** Schematic diagram of the 2 sgRNA target sites at the *GCK* gene locus. The CDS region is indicated by blue rectangles. sgRNA target sites are indicated by green. PAM sites are underlined and highlighted in red. F and R represent the PCR primer pairs used for mutation detection. **b** Mutation detection of F0 *GCK*-NFS rabbits by T7E1 cleavage assay. PCR products of the targeted *GCK* exon 3 region from 12 F0 rabbits (101–112) (upper panel) and their cleavage products (lower panel) are shown. **c** Genomic DNA sequences of the targeted region of *GCK* from the F0 rabbits 101–112, determined by sequencing the cloned PCR products. PAM sites are underlined and highlighted in red; target sequences are green; deletions (−) are shown. *WT* wild type. **d** Computer modeling 3D structure of *GCK* and its fragments. **e** Survival curves of wild type (WT), non-frame shift mutant (*GCK*-NFS) and frame shift mutant (GCK-FS) rabbits. **f** Fasting blood glucose levels of *GCK*-NFS rabbits are shown at the age from 2 to 16 weeks. The data were expressed as the mean ± SEM. A probability of $p < 0.05$ was considered statistically significant. *, $p < 0.05$; **, $p < 0.01$; ***, $p < 0.005$. *ns* not significant

Results

Generation of *GCK* KO rabbits using CRISPR/Cas9

To disrupt open reading frame (ORF) of the *GCK* gene, two sgRNAs targeting the exon 3 of *GCK*, where the most mutant sites have been reported previously in humans [4, 5], were designed using the online tool (http://crispr.mit.edu/) (Fig. 1a). Then, we tested the efficiency of CRISPR/Cas9-mediated gene targeting of the *GCK* gene in rabbit zygotes. As shown in Figure S1A, the microinjected embryos showed similar developmental rates compared to normal embryos. 73.9% of injected embryos developed to the blastocyst stage, and nine of ten blastocysts were found *GCK* mutation (Fig. S1B), demonstrating that the mutations of the *GCK* gene can be achieved via the CRISPR/Cas 9 system with high efficiency in zygotes.

To generate the *GCK* mutant rabbits, 170 injected embryos were transferred to four pseudo-pregnant recipient rabbits. Two of these recipient mothers were pregnant to term and gave birth to 12 live pups (Table 1). Ten of the 12 (83.3%) newborn pups carried a *GCK* mutation with indels ranging from 2 to 36 bp, which was shown by T7E1 assay (Fig. 1b) and confirmed by sequencing of the cloned PCR products (Fig. 1c). Five pups (50%) had a 36 bp deletion with non-frameshift mutation (NFS rabbit). Among them, 2 of 5 are homozygous mutations (#107 and #109, *GCK*-Hom), and others were heterozygosity (#101, #108 and #111, *GCK*-Het). The other 5 (#102, #103, #105, #106, #110) had deletions that lead to a frameshift mutation of *GCK* gene (FS rabbit). The predicted 3D models showed *GCK* protein structures were disrupted in the *GCK* fragment-shift mutation rabbits (GCK-FS rabbit, such as 34 bp and 28 bp deletion) (Fig. 1d). Notably, all *GCK*-FS rabbits died within 12 weeks after birth, and no significantly different survival rate between the *GCK*-NFS and WT rabbits was observed (Fig. 1e).

Furthermore, the potential off-target (POT) effects in these genetically modified rabbits were determined by Sanger sequencing and T7E1, showing that no off-target effects occurred in the *GCK* mutation rabbits (Figure S2). These results demonstrated that cytoplasmic microinjection of dual sgRNA directed CRISPR/Cas9 system efficiently and specifically modified the *GCK* gene in the rabbits in this study.

Typical symptoms of diabetes were found in *GCK*-NFS rabbits

To determine the phenotypes of *GCK*-NFS rabbits, a variety of diabetes-related indicators were compared between WT and *GCK*-NFS rabbits from 2 to 26 weeks. The results showed no significant difference in body weight between the *GCK*-NFS and WT rabbits (Fig. S3A). However, significantly increased fasting blood glucose (Fig. 1f), glucose intolerance (Fig. S3B) and fructosamine levels (Fig. S3C) were found in the *GCK*-NFS rabbits compared to the age-matched WT littermates ($p < 0.05$). Interestingly, the plasma C peptide and insulin levels were also decreased in the *GCK*-NFS rabbits (Fig. S3D and S3E). These results suggested that the *GCK*-NFS rabbits had typical phenotypes of MODY-2-type diabetes, such as a lower insulin level and a higher blood glucose level.

Next, we verified the heritability of the *GCK*-NFS rabbits, the founder (F0) rabbits with 36 bp mutation (#101 and #108) were mated and the genotypes of F1 generation were determined by PCR and sequencing of the PCR products cloned in plasmid. The results showed that 16 of the 26 F1 rabbits carried the 36 bp deletion (6, *GCK*-Hom; 10, *GCK*-Het, 10 *GCK*-WT) (Fig. 2a). As expected, no significant difference of the growth curves was found between the *GCK*-NFS and WT rabbits (Fig. 2b). These results indicated that the *GCK*-NFS rabbits were viable and the targeted mutation of the *GCK* gene is heritable. Therefore, the *GCK*-NFS rabbits can be used for further phenotype analysis and preclinical study as a rabbit model of MODY-2.

We further examined the phenotypes of MODY-2 diabetes in these F1 generation rabbits. As shown in Fig. 2, the F1 *GCK*-NFS mutant rabbits showed similar body weight (Fig.S3A), triglyceride (TG) and total cholesterol (TC) levels (Fig. S3B and S3C) compared to their WT controls, which were consistent with those seen in MODY-2 subjects. Importantly, these rabbits showed increased

Table 1 Generation of genetically *GCK*-targeted rabbits using CRISPR/Cas9

	gRNA/Cas9 mRNA (ng/uL)	Embryos injected	Transferred embryos (% microinjected)	Recipients	Pups obtained (% transferred)	Mutations in the individual (% pups)	Homozygous mutations (% pups)
1	25/100	40	30 (75%)	No			
2	25/100	45	40 (89%)	No			
3	25/100	40	34 (85%)	Yes	5 (12.5%)	4 (80%)	1 (20%)
4	25/100	45	42 (91%)	Yes	7 (15%)	6 (86%)	2 (28.5%)

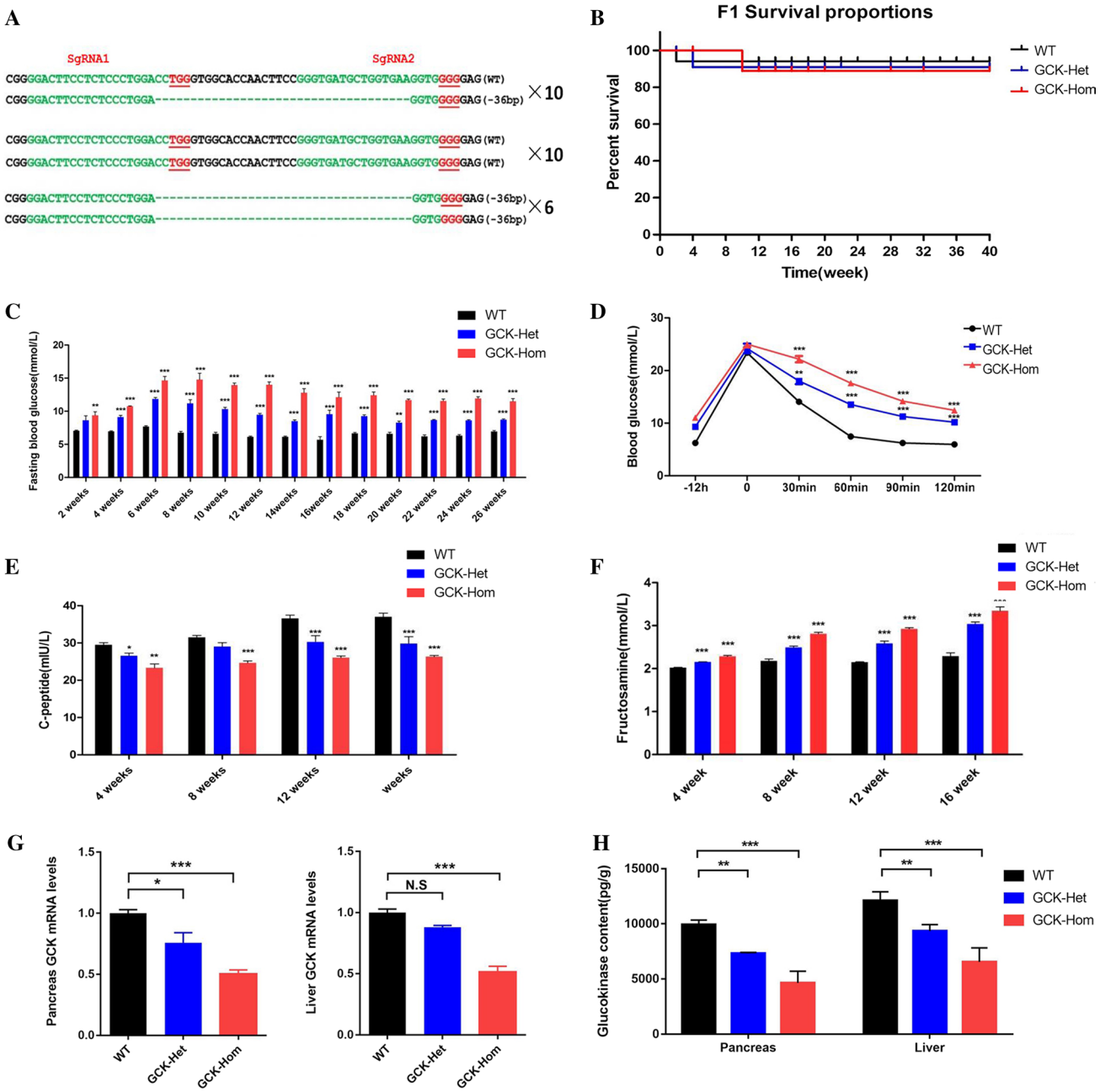

Fig. 2 Phenotype characterization of MODY 2 in F1 *GCK*-NFS rabbits. **a** Sequences of mutant *GCK* gene in F1 rabbits. PAM sites are underlined and highlighted in red; target sequences are green; deletions (−) are shown. *WT* wild type. **b**–**g** Survival curves of wild-type (WT) rabbits and rabbits with *GCK* heterozygous mutation (*GCK*-Het) and homozygous mutation (GCK-Hom) in the F1 generation (**b**), fasting blood glucose (**c**), Intraperitoneal glucose tolerance test result (**d**), blood pro-insulin C peptide level (**e**) and fructosamine (**f**) levels are shown. **g** Relative mRNA levels of of *GCK* gene were determined by qRT-PCR in the pancreas and liver of WT and mutant rabbits and are shown. The data were analyzed by *t* tests using the Graphpad Prism software. **h** Analysis of glucokinase content in pancreas and liver of WT and mutation rabbits. The data were expressed as the mean ± SEM using GraphPad Prism software. A probability of $p < 0.05$ was considered as statistically significant. *, $p < 0.05$; **, $p < 0.01$; ***, $p < 0.005$. *ns* not significant

glycogen content (Fig. 2c), impaired glucose tolerance (Fig. 2d), reduced C peptide expression levels (Fig. 2e) and elevated fructosamine levels (Fig. 2f), which the characteristic changes were seen in the MODY-2 patients.

To determine whether the *GCK* mutation in the rabbits affected the gene expression of *GCK* gene itself, the mRNA level of *GCK* and enzymatic content of glucokinase were examined in liver and pancreas, where glucokinase is mainly

involved in the glycolysis process. As shown in Fig. 2g, h, a significant decrease in both the mRNA levels and enzymatic content was seen in liver and pancreas of the homozygous *GCK-NFS* rabbits when compared with the WT controls, suggesting that the mutant *GCK* products led to the reduction in expression of the *GCK* gene, and a lower glycogen level within the liver and pancreatic cells in these rabbits.

Pancreatic dysfunction in the *GCK*-NFS rabbits

The pancreas contains approximately three million cell clusters called pancreatic islets, which are involved in the regulation of blood glucose (BG) levels [1]. To explore whether the *GCK* gene mutation affected pancreatic function, we firstly examined pathological structure of the pancreatic tissue in the *GCK*-NFS rabbits. The *GCK*-NFS rabbits, both heterozygous and homozygous, displayed a smaller size of islets and weaker staining for insulin compared with WT rabbits as shown by HE staining and insulin immunohistochemical staining (IHC), respectively, on pancreas sections (Fig. 3a). As a result, the levels of circulating insulin in the *GCK*-NFS rabbits were significantly lower than WT rabbits (Fig. 3b). In contrast, glucagon staining was slightly higher in these smaller islets of *GCK*-NFS rabbits (Fig. 3a) and the circulating glucagon levels were increased (Fig. 3c). Moreover, amylopsin and pancrelipase were also decreased in *GCK*-Het rabbits and further decreased in *GCK*-Hom rabbits (Fig. 3d, e), showing a dose-dependent effect of the *GSK* mutation. These pathological changes in pancreas resemble the typical features of human MODY-2 disease, indicating that pancreatic function was affected by glucokinase deficiency and/or the change of the primary structure of GCK with a deletion of 12 amino acid residues.

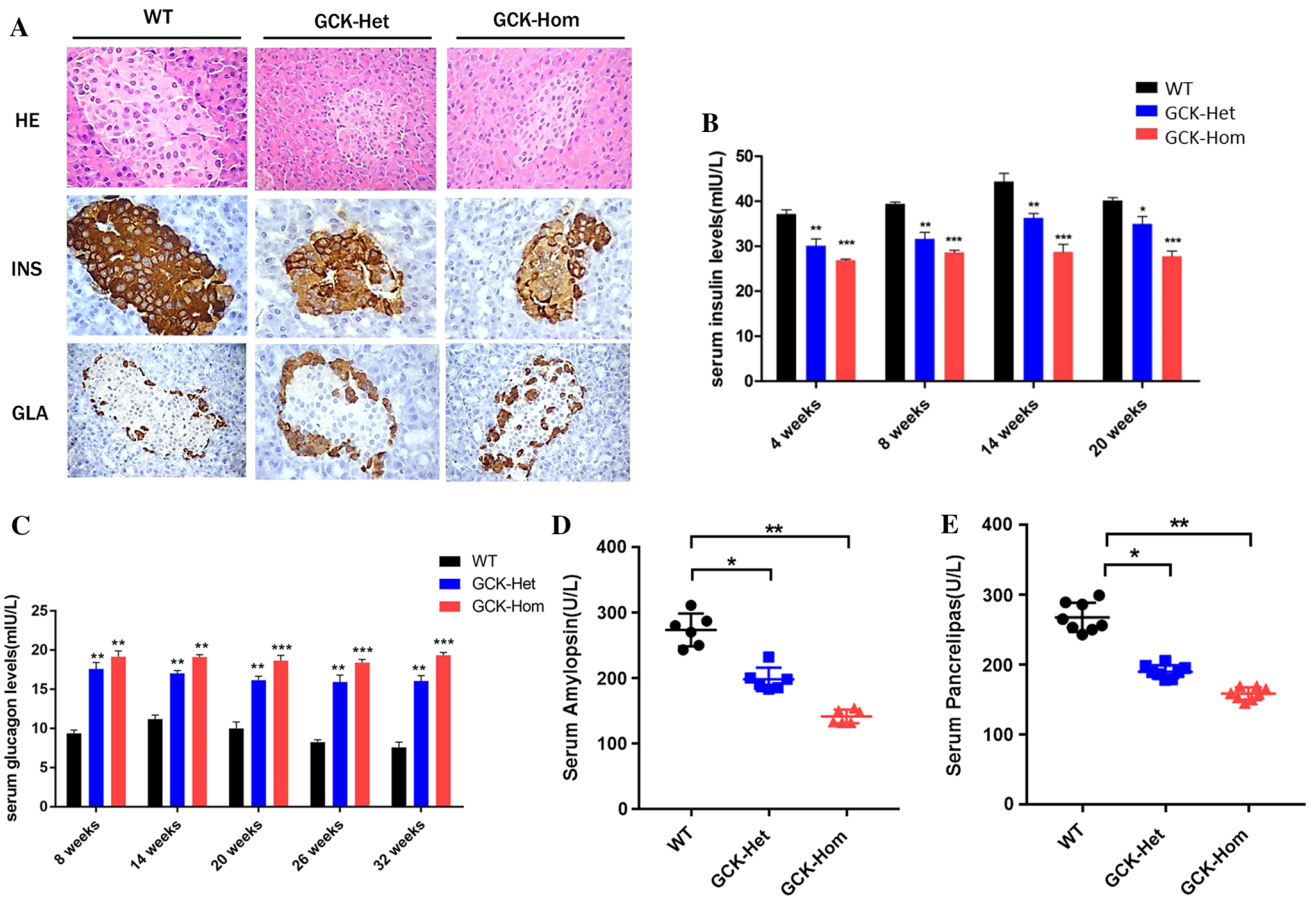

Fig. 3 Pancreatic dysplasia in F1 *GCK*-NFS rabbits. **a** Histological images of the pancreas in WT and *GCK*-NFS rabbits. H.E. staining (HE), immunohistochemical staining (in brown color) for insulin (INS) and glucagon (GLA) are shown. Levels of serum insulin (**b**), serum glucagon (**c**), serum pancreatic amylase (**d**) and serum pancrelipase (**e**) were measured in WT, *GCK*-HET and *GCK*-HOM rabbits in F1 generation. Blood glucose and insulin were measured after a 6-h fasting. The data were expressed as the mean ± SEM. A probability of $p < 0.05$ was considered as statistically significant. *, $p < 0.05$; **, $p < 0.01$; ***, $p < 0.005$. ns, not significant

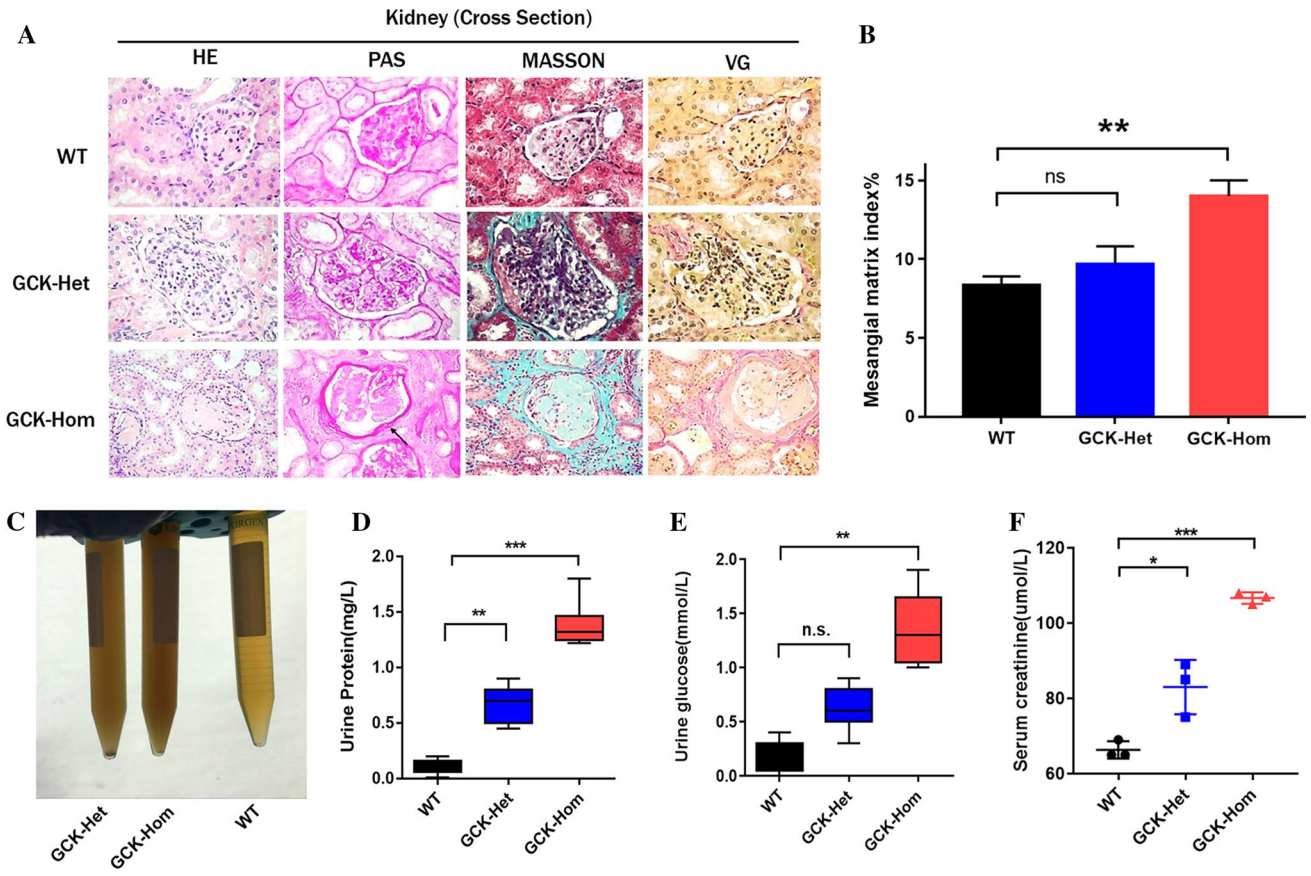

Fig. 4 Renal function is impaired in F1 mutant rabbits. **a** Histological images of kidney from WT and heterozygous (*GCK*-Het) and homozygous (*GCK*-Hom) rabbits are shown. **b** Mesangial matrix index was calculated to quantify differences in the *GCK*-Het and *GCK*-Hom rabbits. *$p<0.05$, **$p<0.01$ vs. age-matched WT rabbits. **c** Photograph of urine samples from WT and *GCK*-NFS rabbits. Urine protein levels (**d**), urine glucose levels (**e**) and serum creatinine levels (**f**) were measured in WT, *GCK*-Het and *GCK*-Hom rabbit in F1 generation. The data were expressed as the mean ± SEM. A probability of $p<0.05$ was considered as statistically significant. *, $p<0.05$; **, $p<0.01$; ***, $p<0.005$. *ns* not significant

Multiple mild diabetic syndrome symptoms in *GCK*-Hom rabbits

Long-term hyperglycemia can result in diabetic complications affecting the eyes, blood vessels, nerves and kidneys in diabetic subjects [28]. In patients of MODY families, typical microvascular and macrovascular complications occur in a frequency similar to those type 2 diabetic patients who have similar levels of hyperglycemia [29, 30]. To determine whether the *GCK*-NFS rabbits developed diabetic complications, the histopathology of multiple tissues was analyzed and compared between *GCK-NFS* and WT rabbits at 8 months of age.

Diabetic nephropathy is one of the most prevalent microvascular complications in diabetic patients with glomerular dysfunctions [31]. As shown in Fig. 4a, b, Masson's trichrome and VG staining of kidney sections showed more extensive renal degeneration and perirenal fibrosis (Fig. 4a), and *GCK-NFS* rabbit displayed significant increase in the amount of mesangial matrix by light microscopy (Fig. 4b). Moreover, we found that the urines of the *GCK-NFS* rabbits were more turbid with significantly increased urine protein and urine glucose in *GCK*-Het rabbits (Fig. 4c) and their parameters further increased in *GCK*-Hom rabbits (Fig. 4e) showing a dose-dependent effect. A similar pattern of elevated serum creatinine levels was seen in heterozygous and homozygous *GCK*-NFS rabbits compared to the WT rabbits (Fig. 4f), suggesting a declined renal function in these rabbits affected by the garget mutation in the *GCK* gene.

Foot disease, which includes infection, ulceration, or destruction of the foot, affects nearly 6% of people with diabetes [32, 33]. In our study, the *GCK*-Hom rabbits exhibited marked ulceration of the superficial layer of the foot at 8 months (Fig. 5a). On the other hand, the histological analysis indicated the myocardium glycogen deposition (PAS stain) and increased fibrosis (Masson's and VG stain) in *GCK*-Hom rabbits (Fig. 5b). Similar pathological alterations

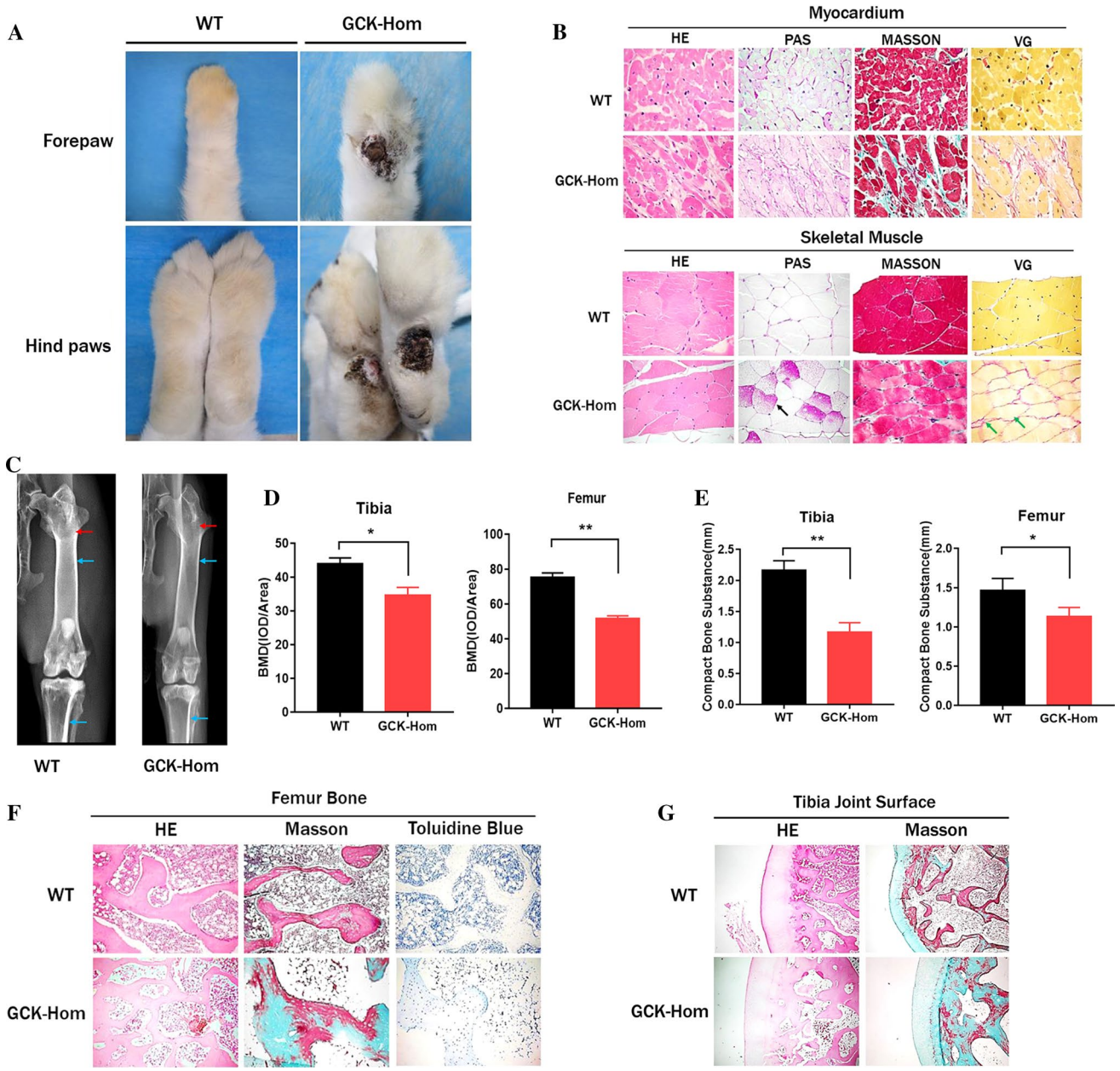

Fig. 5 Pathological observation of multiple organs in F1 mutation rabbits. **a** Superficial ulceration on forepaw and hindpaws of a homozygous *GCK*-NFS rabbit (*GCK*-Hom) and wild-type (WT) rabbits are shown. **b** Histological images of skeletal muscle and myocardium sections of a WT and a homozygous *GCK*-NFS (*GCK*-Hom) rabbit with hematoxylin–eosin staining (HE), periodic acid-Schiff staining (PAS), Masson's trichrome staining (MASSON) and Verhoeff-van Gieson staining (VG) are shown. Black arrow represents glycogen deposition, green arrows represent muscle fiber hyperplasia. **c** X-ray autoradiographs of hindlimbs and forelimbs of 8-month-old WT and *GCK*-Hom rabbit. The blue arrows represent compact bone substance in rabbits. The Red arrows represent bone density. **d** BMD of the Fibula and tibia were analyzed in WT and *GCK*-Hom rabbit. **e** Quantification of the compact bone substance thickness. $*p<0.05$, $**p<0.01$ vs. age-matched WT rabbits. **f**, **g** Pathological section of the fibula (**f**) and osteoarticular (**g**) in WT and *GCK*-Hom rabbit

were also observed in the skeletal muscles, showing more glycogen deposition (Fig. 5b). Therefore, this mutation of the *GCK* gene also led to pathological changes in the foot and muscle of the *GCK*-NFS rabbits.

Finally, we examined the role of *GCK* in osteoblast differentiation and mineralization. Tibia and femur were examined by X-rays imaging analysis (Fig. 5c), which showed a significant reduction in bone density (Fig. 5d) and compact bone substance in *GCK*-Hom rabbit (Fig. 5e). Histological staining showed the typical phenotype of osteoporosis, including bone degeneration, osteoblast reduction and incomplete bone structure, which were also accompanied by bone fibrosis in

GCK-Hom rabbits (Fig. 5f, g). Taken together, these results showed certain levels of injury in multiple sites of the *GCK* mutant rabbits, which represent the complications in association with diabetes mellitus due to the reduction of insulin and disturbance of carbohydrate metabolism.

Drug screening and treatment in *GCK*-NFS rabbits

In most cases, it is considered unnecessary to treat patients with MODY-2 since they usually have mild hyperglycemia which rarely led to serious complications. However, MODY-2-type diabetes occurring in middle-aged and older people, as well as during pregnancy, requires treatment [34]. The current strategy for treating Type-1 and most Type-2 diabetes mellitus is insulin therapy and oral hypoglycemics [35, 36]. As a proof-of-principle study, we explored to treat these *GCK*-NFS rabbits as a model of MODY-2 with anti-diabetic medicines.

Firstly, we measured the effects of glimepiride in *GCK*-NFS rabbits. Drug concentration screening test showed that glimepiride at 0.2 mg/kg can reduce the BG level moderately in 4 h and continue to 24 h after injection in both WT and *GCK* mutant rabbits (Fig. 6a, b). Moreover, the similar treatment effect had been verified on repaglinide at 0.1 mg/kg (Fig. 6c) and insulin at 5 U/kg (Fig. 6d) in *GCK* mutant rabbits. Surprisingly, no effect was observed with Metformin and Sitagliptin, even if we increased the concentration to 0.4 mg/kg (Fig. S5A and S5B), suggesting that insulin, glimepiride and repaglinide are efficacious to reduce the symptoms resulted from an abnormal *GCK* as seen in MODY-2.

To evaluate the long-term effects of glimepiride in the *GCK-NFS* rabbits, we treated the *GCK-NFS* rabbits with daily oral administration of glimepiride (0.2 mg/kg) for 28 days. The BG levels were significant monotonic decrease in the *GCK*-Hom rabbits treated with glimepiride (*GCK*-Hom^{Glim}) (Fig. 6e). Similarly, the insulin and C peptide concentrations in plasma were significantly increased to normal level (Fig. 6f, g). Histological analysis revealed reduced glycogen deposition in skeletal muscle, and significantly increased insulin-positive islet cells in the pancreas of *GCK*-Hom^{Glim} rabbits receiving glimepiride treatment (Fig. 6h, i). These results provided experimental evidence that glimepiride can be used to treat MODY-2 subjects with symptoms of diabetes mellitus, thus highlighting the usefulness of our *GCK*-NFS rabbit model for preclinical studies.

Discussion

Glucokinase encoded by the *GCK* gene is the main glucose-phosphorylating enzyme in the liver and pancreatic beta cells. It converts glucose into G6P as a first and rate-limiting step in glycolysis, which plays a part in the process of glucose oxidation [15, 16]. In previous studies, the heterozygous *Gck* KO mice were hyperglycemic and the *Gck* null mice were lethal either at midgestation [6], or a few days after birth [7]. Approximately, one-third of the embryos in timed pregnancies were found to be reabsorbed starting at E9.5, indicating that the absence of *Gck* is lethal to embryos [16]. In our study, all the *GCK*-FS rabbits with the *GCK* gene disrupted at exon 3 died within 12 weeks after birth (Fig. 1e). We speculated that the reason for the prolonged survival may be that they were chimeras, which were common in CRISPR/Cas9 embryonic injections because genome editing occurs following the one-cell embryonic stage, resulting in diverse genetic outcomes [37, 38]. Fortunately, different from *Gck* KO mice, the *GCK*-NFS rabbits are fertile which showed the typical characteristics of diabetes similar to the MODY-2 in man. Therefore, the *GCK*-NFS rabbit is likely useful in preclinical studies to evaluate the therapeutic effects of new treatment. The relatively lower maintenance cost and shorter gestational duration make the *GCK*-NFS rabbit a particularly attractive model for preclinical studies.

It is worth noting that the homozygous *GCK* mutant rabbits exhibited more severe diabetic symptoms, including a greater degree of hyperglycemia (Fig. 2c), lower insulin level in the circulation (Fig. 3b) and various complications associated with diabetes (Figs. 4, 5). These changes are consistent with the significant decrease in the glucokinase enzymatic activity compared with *GCK*-Het and WT rabbits. On the other hand, it is understood that *GCK* can send signal to release insulin from β cells when blood glucose level increased, whereas MODY2 mutant *GCK* has an increased threshold of blood glucose sensing [39]. Therefore, we speculate that the 36bp deleted fragment at exon 3 of the *GCK* gene may be involved in blood glucose sensing. The deletion of this fragment within glucokinase leads to an increased threshold of blood glucose sensing and consequent hyperglycemia, accompanied by the decrease of insulin levels in the circulation.

Creatinine is a metabolic product of creatine and phosphocreatine, and excreted through glomerular filtration, which is both found almost exclusively in muscle [40]. Thus, creatinine production is proportional to muscle mass and varies little from day to day when kidney filtration function is normal [41]. The concentration of blood creatinine reflects the functional status of glomerular filtration. When the glomerular filtration rate (GFR) decreases to a critical level (typically 1/3 of the normal level), serum creatinine concentration increases dramatically; therefore, it is considered to be an indicator of GFR impairment, although not useful for early diagnosis. The blood creatinine levels were found to be increased in the *GCK-NFS* rabbits which have spontaneous diabetes, suggesting that

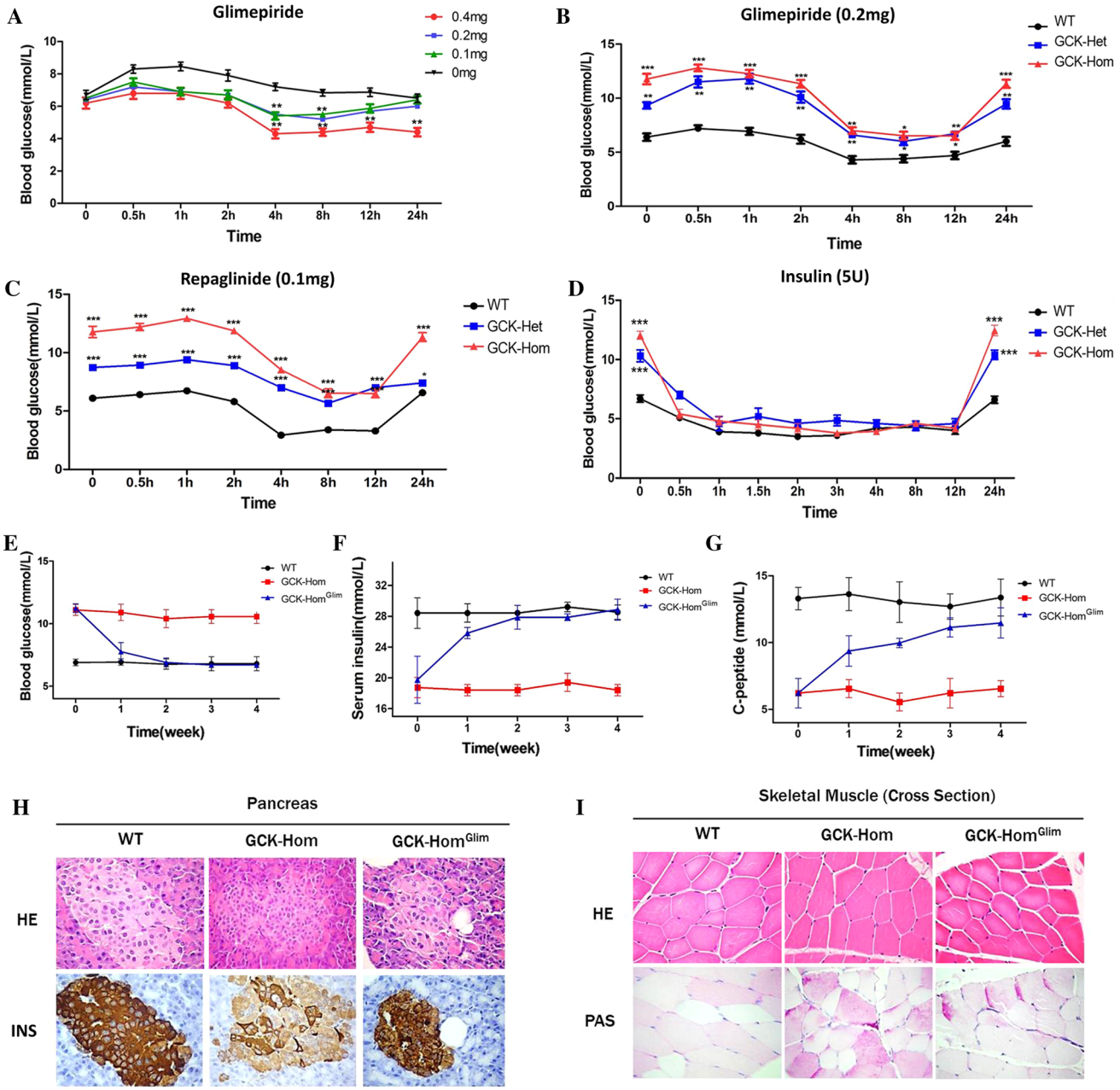

Fig. 6 Drug screening and treatment in *GCK*-NFS rabbits. **a** Fasting blood-glucose levels in WT rabbits at specified time points after treatment with glimepiride at various doses. **b** Fasting blood-glucose levels in WT, GCK-Het and GCK-Hom rabbits at various time points after a treatment with glimepiride at 0.2 mg. **c**–**f** Fasting blood-glucose levels in WT, *GCK*-Het and *GCK*-Hom mutant rabbits at various time points after a treatment with 0.1 mg repaglinide (**c**), 5 IU insulin (**d**) are shown. The data are expressed as the mean ± SEM. A probability of $p < 0.05$ was considered as statistically significant. *, $p < 0.05$; **, $p < 0.01$; ***, $p < 0.005$. *ns* not significant. **e**–**g** Weekly levels of blood glucose (**e**), serum insulin (**f**) and serum C peptide (**g**) were measured in WT, *GCK*-Hom rabbits and *GCK*-Hom rabbits treated with glimepiride at 0.2 mg daily are shown for 4 weeks. Glucose and insulin were measured after a 6-h fasting. The data were expressed as the mean ± SEM. A probability of $p < 0.05$ was considered statistically significant. *, $p < 0.05$; **, $p < 0.01$; ***, $p < 0.005$. *ns* not significant. **d**, **e** Histological images of pancreas (**d**) and skeletal muscle € from a WT and a GCK-Hom rabbit and a GCK-Hom rabbit receiving glimepiride treatment for 4 weeks are shown. Tissue sections were stained by hematoxylin–eosin staining (HE), immunohistochemical staining of insulin (INS) or periodic acid-Schiff staining (PAS)

these rabbits have impaired renal function, an important complication of diabetes.

Diabetes is a chronic condition requiring long-term treatment to control the blood glucose levels, with both hyperglycemia and hypoglycemia leading to severe health consequences. As such, methods of treating the condition must be able to be readily maintained over a long period of time. In this paper, we show that both glimepiride and repaglinide have a significant effect to reduce blood glucose levels in the *GCK*-NFS rabbits (Fig. 6). These drugs are anti-diabetic medicines for Type-2 DM. They lower blood glucose levels by stimulating the release of insulin from pancreatic β-cells and have antioxidant and hypolipidemic actions as well [42, 43]. The efficacious effects of these drugs in the GCK-NFS rabbits are consistent with our finding that these rabbits had reduced insulin levels, which led to hyperglycemia.

However, there is no effect observed in the *GCK*-NFS rabbits receiving Metformin and Sitagliptin treatment (Fig. S5A and S5B). Sitagliptin is a selective DPP-4 inhibitor that enhances intact (active) incretin levels and improves 24-h glycemic control in patients with type 2 diabetes and Metformin is a biguanide that decreases blood glucose concentration by mechanisms different from those of sulphonylurea or insulin [44]. Although it is generally agreed that metformin reduces fasting plasma glucose concentrations by reducing rates of hepatic glucose production [45], its effect on the relative contributions of hepatic glycogenolysis and gluconeogenesis remains controversial. Some studies conclude that metformin works mostly by reducing rates of gluconeogenesis [43]. These findings support that the insulin insufficiency in the circulation is likely the major mechanism underlying the hyperglycemia in these mutant rabbits, and if this is the case in MODY-2, sitagliptin and biguanide drugs may not be suitable for treating MODY-2-type patients.

Our finding that the pancreatic islets are reduced in size with decreased insulin expression levels in both islets and the circulation in the GCK-NFS rabbits may have a significant clinical significance. These changes are caused as a result of deletion of a 12-residue fragment of glucokinase, suggesting that MODY-2 patients, particularly those with mutations within this region of *GCK* gene, require monitoring of their β-cell function and insulin levels. Furthermore, these results suggest a potential biological function of the glucokinase domain containing the 12-residue fragment in regulating expression of insulin gene as well as blood glucose sensing.

To the best of our knowledge, this is the first report of recapitulation of the typical symptoms of MODY-2 in rabbit by a CRISPR/Cas9 approach. This new model would facilitate basic research to understand the pathogenesis of MODY-2 and the translational studies to develop novel therapeutic strategies for this disease.

Acknowledgements The authors thank Peiran Hu for excellent technical assistance at the Embryo Engineering Center. This study was financially supported by the National Key Research and Development Program of China Stem Cell and Translational Research (2017YFA0105101). The Strategic Priority Research Program of the Chinese Academy of Sciences (XDA16030501, XDA16030503), Guangdong Province science and technology plan project (2014B020225003). China Postdoctoral Science Foundation Funded Project (2018M641784). China Postdoctoral Science Foundation Funded Project (2018M641784).

Compliance with ethical standards

Conflict of interest No conflict of interest to disclose.

References

1. Ellard S, Bellanne-Chantelot C, Hattersley AT, European Molecular Genetics Quality Network MG (2008) Best practice guidelines for the molecular genetic diagnosis of maturity-onset diabetes of the young. Diabetologia 51:546–553
2. Matschinsky F, Liang Y, Kesavan P, Wang L, Froguel P, Velho G, Cohen D, Permutt MA, Tanizawa Y, Jetton TL et al (1993) Glucokinase as pancreatic beta cell glucose sensor and diabetes gene. J Clin Investig 92:2092–2098
3. Dimitriadis G, Boutati E, Raptis SA (2007) The importance of adipose tissue in diabetes pathophysiology and treatment. Hormone Metab Res 39:705–706
4. Stenson PD, Mort M, Ball EV, Howells K, Phillips AD, Thomas NS, Cooper DN (2009) The human gene mutation database: 2008 update. Genome Med 1:13
5. Osbak KK, Colclough K, Saint-Martin C, Beer NL, Bellanne-Chantelot C, Ellard S, Gloyn AL (2009) Update on mutations in glucokinase (GCK), which cause maturity-onset diabetes of the young, permanent neonatal diabetes, and hyperinsulinemic hypoglycemia. Hum Mutat 30:1512–1526
6. Bali D, Svetlanov A, Lee HW, Fusco-DeMane D, Leiser M, Li B, Barzilai N, Surana M, Hou H, Fleischer N et al (1995) Animal model for maturity-onset diabetes of the young generated by disruption of the mouse glucokinase gene. J Biol Chem 270:21464–21467
7. Grupe A, Hultgren B, Ryan A, Ma YH, Bauer M, Stewart TA (1995) Transgenic knockouts reveal a critical requirement for pancreatic beta cell glucokinase in maintaining glucose homeostasis. Cell 83:69–78
8. Terauchi Y, Sakura H, Yasuda K, Iwamoto K, Takahashi N, Ito K, Kasai H, Suzuki H, Ueda O, Kamada N et al (1995) Pancreatic beta-cell-specific targeted disruption of glucokinase gene. Diabetes mellitus due to defective insulin secretion to glucose. J Biol Chem 270:30253–30256
9. Ferre T, Pujol A, Riu E, Bosch F, Valera A (1996) Correction of diabetic alterations by glucokinase. Proc Natl Acad Sci USA 93:7225–7230
10. Ferre T, Riu E, Bosch F, Valera A (1996) Evidence from transgenic mice that glucokinase is rate limiting for glucose utilization in the liver. FASEB J 10:1213–1218
11. Hariharan N, Farrelly D, Hagan D, Hillyer D, Arbeeny C, Sabrah T, Treloar A, Brown K, Kalinowski S, Mookhtiar K (1997) Expression of human hepatic glucokinase in transgenic mice liver results in decreased glucose levels and reduced body weight. Diabetes 46:11–16
12. Niswender KD, Postic C, Jetton TL, Bennett BD, Piston DW, Efrat S, Magnuson MA (1997) Cell-specific expression and

regulation of a glucokinase gene locus transgene. J Biol Chem 272:22564–22569
13. Zhang YL, Tan XH, Xiao MF, Li H, Mao YQ, Yang X, Tan HR (2004) Establishment of liver specific glucokinase gene knockout mice: a new animal model for screening anti-diabetic drugs. Acta Pharmacol Sin 25:1659–1665
14. Gu Y, Mao Y, Li H, Zhao S, Yang Y, Gao H, Yu J, Zhang X, Irwin DM, Niu G et al (2011) Long-term renal changes in the liver-specific glucokinase knockout mouse: implications for renal disease in maturity-onset diabetes of the young 2. Transl Res 157:111–116
15. Postic C, Shiota M, Magnuson MA (2001) Cell-specific roles of glucokinase in glucose homeostasis. Recent Prog Horm Res 56:195–217
16. Postic C, Shiota M, Niswender KD, Jetton TL, Chen Y, Moates JM, Shelton KD, Lindner J, Cherrington AD, Magnuson MA (1999) Dual roles for glucokinase in glucose homeostasis as determined by liver and pancreatic beta cell-specific gene knock-outs using Cre recombinase. J Biol Chem 274:305–315
17. Bosze Z, Hiripi L, Carnwath JW, Niemann H (2003) The transgenic rabbit as model for human diseases and as a source of biologically active recombinant proteins. Transgenic Res 12:541–553
18. Wang Y, Fan N, Song J, Zhong J, Guo X, Tian W, Zhang Q, Cui F, Li L, Newsome PN et al (2014) Generation of knockout rabbits using transcription activator-like effector nucleases. Cell Regen 3:3
19. Song Y, Yuan L, Wang Y, Chen M, Deng J, Lv Q, Sui T, Li Z, Lai L (2016) Efficient dual sgRNA-directed large gene deletion in rabbit with CRISPR/Cas9 system. Cellular Mol Life Sci CMLS 73:2959–2968
20. Song Y, Liu T, Wang Y, Deng J, Chen M, Yuan L, Lu Y, Xu Y, Yao H, Li Z et al (2017) Mutation of the Sp1 binding site in the 5' flanking region of SRY causes sex reversal in rabbits. Oncotarget 8:38176–38183
21. Yuan L, Yao H, Xu Y, Chen M, Deng J, Song Y, Sui T, Wang Y, Huang Y, Li Z et al (2017) CRISPR/Cas9-mediated mutation of alphaA-crystallin gene induces congenital cataracts in rabbits. Investig Ophthalmol Visual Sci 58:BIO34–BIO41
22. Hayashi H, Sato Y, Li Z, Yamamura K, Yoshizawa T, Yamagata K (2015) Roles of hepatic glucokinase in intertissue metabolic communication: examination of novel liver-specific glucokinase knockout mice. Biochem Biophys Res Commun 460:727–732
23. Guschin DY, Waite AJ, Katibah GE, Miller JC, Holmes MC, Rebar EJ (2010) A rapid and general assay for monitoring endogenous gene modification. Methods Mol Biol 649:247–256
24. Latti BR, Birajdar SB, Latti RG (2015) Periodic acid schiff-diastase as a key in exfoliative cytology in diabetics: a pilot study. J Oral Maxillofac Pathol JOMFP 19:188–191
25. Gruber HE (1992) Adaptations of Goldner's Masson trichrome stain for the study of undecalcified plastic embedded bone. Biotech Histochem 67:30–34
26. Bergmann B, Molne J, Gjertsson I (2015) The bone-inflammation-cartilage (BIC) stain: a novel staining method combining Safranin O and Van Gieson's Stains. J Histochem Cytochem 63:737–740
27. Awale R, Maji R, Patil P, Lingiah R, Mukhopadhyay AK, Sharma S (2017) Toluidine blue: rapid and simple malaria parasite screening and species identification. Pan Afr Med J 28:27
28. Iynedjian PB (1993) Mammalian glucokinase and its gene. Biochem J 293(Pt 1):1–13
29. Fajans SS (1990) Scope and heterogeneous nature of MODY. Diabetes Care 13:49–64
30. Fajans SS (1987) MODY—a model for understanding the pathogeneses and natural history of type II diabetes. Hormone Metab Res 19:591–599
31. Zerbini G, Maestroni S, Turco V, Secchi A (2017) The eye as a window to the microvascular complications of diabetes. Dev Ophthalmol 60:6–15
32. Mishra SC, Chhatbar KC, Kashikar A, Mehndiratta A (2017) Diabetic foot. BMJ 359:j5064
33. Raghav A, Khan ZA, Labala RK, Ahmad J, Noor S, Mishra BK (2018) Financial burden of diabetic foot ulcers to world: a progressive topic to discuss always. Therap Adv Endocrinol Metab 9:29–31
34. Bennett K, James C, Mutair A, Al-Shaikh H, Sinani A, Hussain K (2011) Four novel cases of permanent neonatal diabetes mellitus caused by homozygous mutations in the glucokinase gene. Pediatr Diabetes 12:192–196
35. Yki-Jarvinen H (2001) Combination therapies with insulin in type 2 diabetes. Diabetes Care 24:758–767
36. American Diabetes A (2000) Implications of the United Kingdom prospective diabetes study. Diabetes Care 23(Suppl 1):S27–31
37. Singh P, Schimenti JC, Bolcun-Filas E (2015) A mouse geneticist's practical guide to CRISPR applications. Genetics 199:1–15
38. Yen ST, Zhang M, Deng JM, Usman SJ, Smith CN, Parker-Thornburg J, Swinton PG, Martin JF, Behringer RR (2014) Somatic mosaicism and allele complexity induced by CRISPR/Cas9 RNA injections in mouse zygotes. Dev Biol 393:3–9
39. Fajans SS, Bell GI (2011) MODY: history, genetics, pathophysiology, and clinical decision making. Diabetes Care 34:1878–1884
40. Brenner D, Gerstberger R (1999) Functional receptors in the avian kidney for C-type natriuretic peptide. Endocrinology 140:1622–1629
41. Heymsfield SB, Arteaga C, McManus C, Smith J, Moffitt S (1983) Measurement of muscle mass in humans: validity of the 24-h urinary creatinine method. Am J Clin Nutr 37:478–494
42. Derosa G, Gaddi AV, Piccinni MN, Salvadeo S, Ciccarelli L, Fogari E, Ghelfi M, Ferrari I, Cicero AF (2006) Differential effect of glimepiride and rosiglitazone on metabolic control of type 2 diabetic patients treated with metformin: a randomized, double-blind, clinical trial. Diabetes Obes Metab 8:197–205
43. Wang M, Gao F, Xue YM, Han YJ, Fu XJ, He FY (2011) Effect of short-term intensive therapy with glimepiride and metformin in newly diagnosed type 2 diabetic patients. Nan fang yi ke da xue xue bao J South Med Univ 31:564–566
44. Bailey CJ, Turner RC (1996) Metformin. N Engl J Med 334:574–579
45. Cusi K, Consoli A, DeFronzo RA (1996) Metabolic effects of metformin on glucose and lactate metabolism in noninsulin-dependent diabetes mellitus. J Clin Endocrinol Metab 81:4059–4067